© MAY 2026 | IRE Journals | Volume 9 Issue 11 | ISSN: 2456-8880
DOI: https://doi.org/10.64388/IREV9I11-1717515

Induction Motor Drive by Voltage Source Inverter (VSI)

ONAH, A.J.[1], EZEMA, E.E.[2], EJIMOFOR I. A[3]

[1]*Department of Electrical/Electronic Engineering, College of Engineering & Engineering Technology, Michael Okpara University of Agriculture, Umudike, Abia State, Nigeria.*

[2]*Department of Electrical/Electronic Engineering, Faculty of Engineering, Madonna University, Nigeria.*

[3]*Department of Computer Engineering, Faculty of Engineering, Madonna University, Nigeria.*

Abstract- ***Induction motor is cheap, rugged, reliable, and long-lasting compared to the dc motor. It requires little maintenance because of the absence of commutator and brushes, and can be operated in explosive and contaminated surroundings. The volume, weight, and inertia are lower, while the operational speed, voltage and power can be made higher than in dc motors. The electric drive systems used in industrial applications are increasingly required to meet higher performance and reliability. Hence about ninety percent of all industrial motor applications are induction motors. The load on induction motor is not constant, and varies as per load requirement. So speed and torque must change as per load. This paper investigates variable frequency drive of induction motor, employing power semiconductor converters. The speed and torque of the induction motor are controlled by either the stator supply frequency ( ), or stator voltage ( ). Advances in power electronics has made variable frequency drives popular. The converters used here are controlled rectifier and voltage source inverter (VSI). Controlled rectifier is used to provide controlled dc input voltage to the inverter, which converts the dc voltage to variable frequency ac voltage, feeding the induction motor. So the control scheme is an ac-to-ac converter with a dc link.***

Keywords: induction motor, speed control, variable frequency control, controlled rectifier, voltage source inverter

I. INTRODUCTION

Induction motors are widely used in many residential, commercial, industrial and utility applications. This is because the motor has low manufacturing costs, wide speed range, high efficiency and robustness (Arbi et al., 2012; John et al, 1998; Federico C. and Onorato, 1998). Induction motors, both three- and single-phase, are used extensively for adjustable-speed drives applications. Actually, induction machines dominate the scene of adjustable-speed pump drives because of the cost-driven nature of such motor application (Katsumi and Yoshihisa, 2004; Hubert et al, 2004). This paper investigates the control of three-phase induction motor by voltage source inverter (VSI), fed by three-phase controlled rectifier. The speed of the induction motor is controlled by any of the following methods: (i) varying the stator voltage, , (ii) varying the supply frequency, , which controls the synchronous speed (and, hence, the motor speed), (iii) keeping the flux, ϕ constant by varying in a linear proportion to (Dubey, 1989; Muhammad, 1993). So, different operating zones for various speeds and torques are obtained. Thus, variable frequency control is employed to achieve efficient motor breaking and speed reversal, and to reduce the starting current. The output frequency of the inverter is controlled by changing the switching frequency, and the magnitude of the output voltage is determined by the value of the dc supply voltage. So the dc input is adjusted in order to control the output voltage of the six-step inverter, which feeds the induction motor. The scheme employs a controlled rectifier for getting the variable dc voltage. An LC filter is interposed between the rectifier and the inverter in order to keep the dc voltage ripple-free, and thus prevent the harmonics at the rectifier output voltage from interfering with the inverter, and the harmonics in the inverter input current from interfering with the rectifier (Miller et al, 2004; Roozbeh et al, 2016).

II. MATERIALS AND METHOD.

2.1. Semiconductor Converters

The schematic of the induction motor drive is shown in Figure 1. It is an ac-to-ac converter with a dc link.

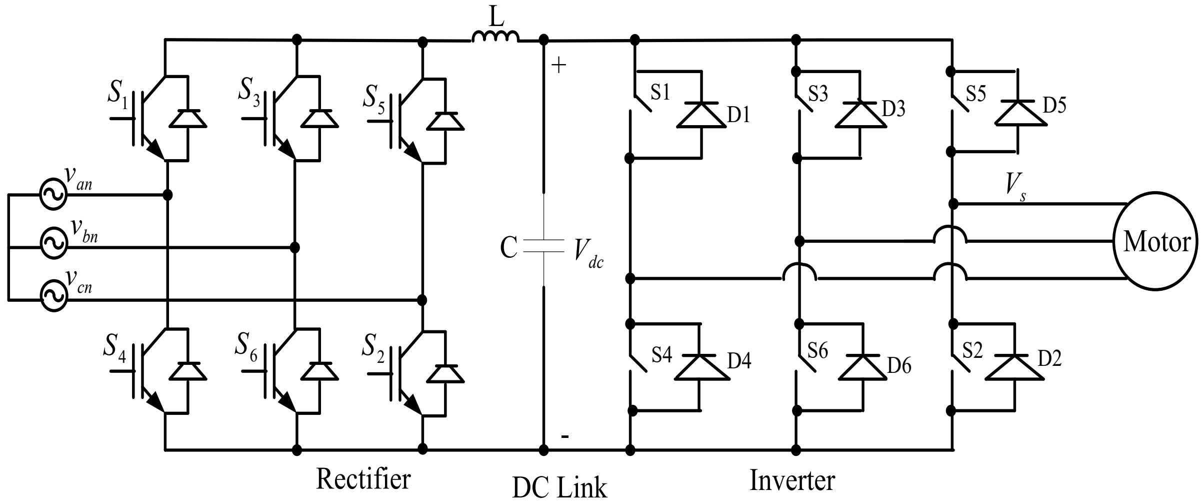

Figure 1: Voltage Source Inverter Induction Motor Drive

The average output voltage of the rectifier is given by:

$$V_o = \frac{1}{\pi/3}\int_{\frac{\pi}{3}+\alpha}^{\frac{2\pi}{3}+\alpha} V_m \sin\omega t d\omega t = \frac{3V_m}{\pi}\int_{\frac{\pi}{3}+\alpha}^{\frac{2\pi}{3}+\alpha} \sin\omega t\, d\omega t = \frac{3V_m}{\pi}\cos\alpha \quad (1)$$

Maximum output voltage, $V_{o\max} = \frac{3V_m}{\pi}$

The rms output voltage is:

$$V = \left[\frac{1}{\pi/3}\int v_{ab}^2 d\omega t\right]^{\frac{1}{2}} = \left[\frac{3}{\pi}\int_{\frac{\pi}{3}+\alpha}^{\frac{2\pi}{3}+\alpha} V_m^2 \sin^2\omega t\, d\omega t\right]^{\frac{1}{2}} = V_m\left[\frac{1}{2}+\frac{3\sqrt{3}\cos 2\alpha}{4\pi}\right]^{\frac{1}{2}} \quad (2)$$

It is obvious from equation (1) that variable dc voltage, V_{dc} (rectifier output voltage, V_o) is obtained by adjusting the delay angle (α) of the rectifier switches. The magnitude of the inverter output voltage depends on V_{dc}.

The line-to-line output voltage of the inverter can be shown to be:

$$v_{ab} = \sum_{n=1,5,7}^{\infty} \frac{4V_{dc}}{n\pi}\cos\frac{n\pi}{6}\sin\left(n\omega t + \frac{n\pi}{6}\right) \quad (3)$$

Where $V_{dc} = V_o$

DOI: https://doi.org/10.64388/IREV9I11-1717515

The rms value of the fundamental of v_{ab} is $\frac{\sqrt{6}\,V_{dc}}{\pi}$. v_{ab} is plotted as shown in Figure 2

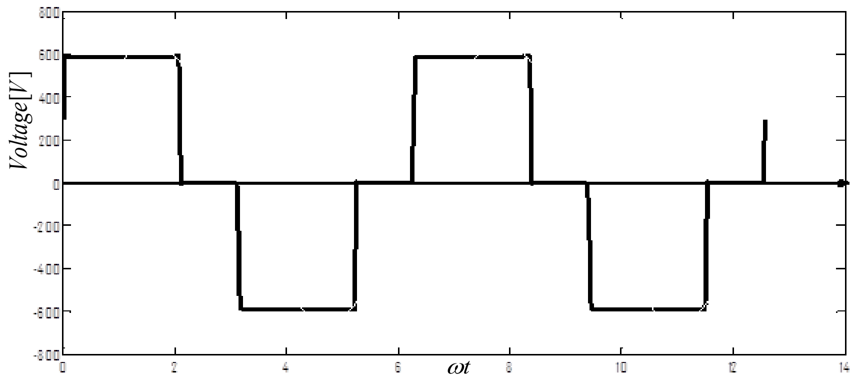

Figure 2: Line-to-line output voltage (v_{ab}) waveform of three-phase inverter

Line-to-neutral voltage can be shown to be:

$$v_{an} = \sum_{n=6p\pm 1}^{\infty} \frac{2V_{dc}}{n\pi} \sin n\omega t \tag{4}$$

$p = 1, 2, 3, \ldots$

The rms value of the fundamental of v_{an} is $\frac{\sqrt{2}\,V_{dc}}{\pi}$. The Line-to-neutral voltage, v_{an} , and the motor input current (i_s) in phase-a are shown in Figure 3. The induction motor is rated as: 460-V, 60-Hz, 6-pole, 1180-rpm, and Y – connected. The parameters per phase referred to the stator are: $R_s = 0.19\,\Omega$, $R_r^{'} = 0.07\,\Omega$, $X_s = 0.75\,\Omega$ $X_r^{'} = 0.67\,\Omega$, and $X_m = 20\,\Omega$.

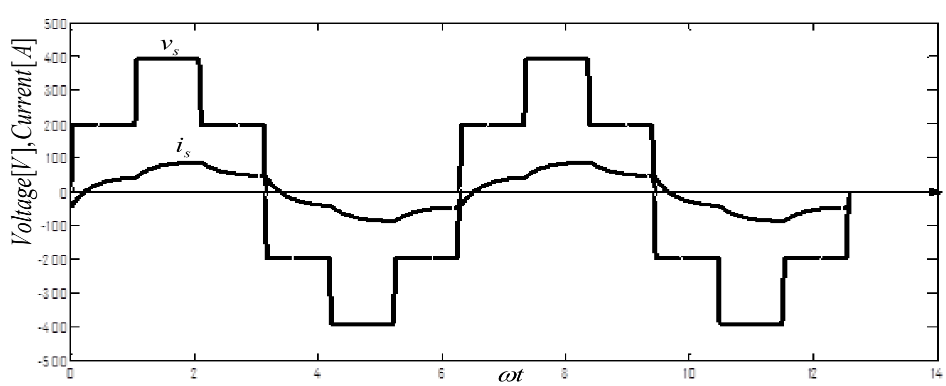

Figure 3: Six-step output voltage of the three-phase inverter (motor input voltage) and current ( )

© MAY 2026 | IRE Journals | Volume 9 Issue 11 | ISSN: 2456-8880
DOI: https://doi.org/10.64388/IREV9I11-1717515

2. 2 Induction Motor

The rotor bars are shorted to represent squirrel cage induction motor, or it is wound rotor with shorted terminals. Three-phase squirrel cage induction motors in particular is by far the most representative of the rotating electrical machines used in the present industrial driven equipment because of its roughness and versatility (Miller et al, 2004). These machines are structurally very robust and are a primary source of motive power and speed control where dc machines cannot be used (Subhasis et al, 2003). The equivalent circuit of the induction motor is shown in Figure 4.

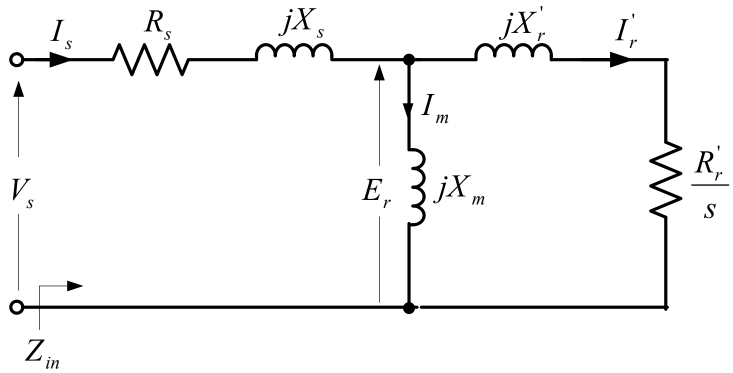

Figure 4: Per-phase equivalent circuit

$$Z_{in} = R_s + jX_s + \frac{jX_m\left(\frac{R_r'}{s} + jX_r'\right)}{\frac{R_r'}{s} + j\left(X_m + X_r'\right)} \tag{5}$$

$$I_s = \frac{V_s}{Z_{in}} \tag{6}$$

$$I_r' = \frac{jX_m I_s}{\frac{R_r'}{s} + j\left(X_r' + X_m\right)} \tag{7}$$

The airgap power is the power dissipated in rotor resistance $\frac{R_r'}{s}$

$$P_a = 3I_r'^2 \frac{R_r'}{s} \tag{8}$$

Rotor copper loss, $P_{rcu} = 3I_r'^2 R_r'$

This is subtracted from P_a to get mechanical output power P_m given by:

$$P_m = P_a - P_{rcu} = 3I_r'^2 \frac{R_r'}{s} - 3I_r'^2 R_r' = 3I_r'^2 \frac{R_r'}{s}\left(1-s\right) \tag{9}$$

Synchronous speed is given by:

© MAY 2026 | IRE Journals | Volume 9 Issue 11 | ISSN: 2456-8880
DOI: https://doi.org/10.64388/IREV9I11-1717515

$$\omega_s = \frac{2}{p}\omega = \frac{2}{p}2\pi f = \frac{4\pi f}{p} \tag{10}$$

Where *f* is the stator supply frequency and *p* is number of poles.

The motor speed, ω_m is derived from the definition of slip *s* as:

$$s = \frac{\omega_s - \omega_m}{\omega_s} = \frac{\frac{2}{p}\omega - \omega_m}{\frac{2}{p}\omega} \tag{11}$$

$$\omega_m = \frac{2}{p}\omega(1-s) \tag{12}$$

Developed motor torque, T_m is:

$$T_m = \frac{P_m}{\omega_m} = \frac{3p}{2\omega}\frac{R_s}{s}I_r'^2 \tag{13}$$

At synchronous speed, $s = 0$, and $T_m = 0$.

III. RESULTS AND DISCUSSION

3.1 Stator Voltage Control.

Equation (13) shows that the torque developed by an induction motor is proportional to the square of the rotor current, which is proportional to the square of the stator supply voltage, ( ). The speed of the motor is controlled by varying until the torque required by the load is developed at the desired speed (Domentico et al, 2003; Nkosinathi and Maarten, 2014). This method of speed control is applied only below rated speed since voltage ( ) above rated value must not be applied to the motor. is varied by adjusting the delay angle, of the rectifier switches. So, decrease in results in reduction of speed and torque. Let be decreased to , where . The equivalent circuit referred to the stator is shown in Figure 5.

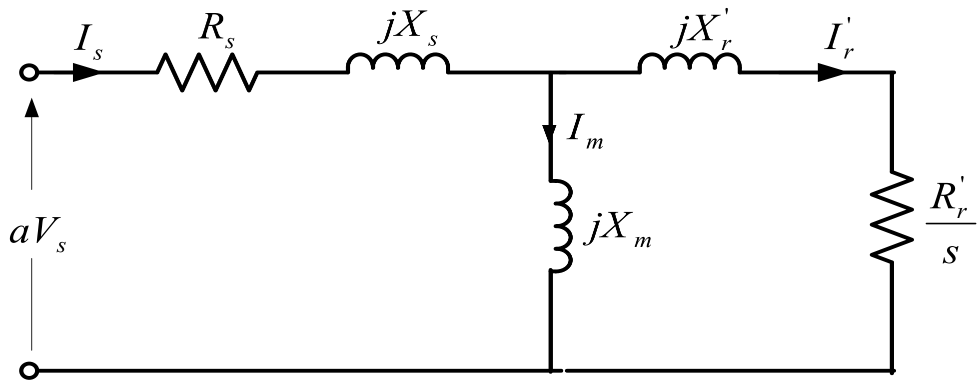

Figure 5: Per phase equivalent circuit referred to the stator

From Figure 7

$$I_s = \frac{aV_s}{Z_{in}} \tag{14}$$

$$I_r' = \frac{jX_m I_s}{\frac{R_r'}{s} + j\left(X_r' + X_m\right)} \tag{15}$$

$$\omega_m = \frac{2}{p}\omega\left(1 - s\right) \tag{16}$$

$$T_m = \frac{3p}{2\omega}\frac{R_s}{s} I_r'^2 \tag{17}$$

Figure 6 shows the typical torque - speed characteristics for various values of a .

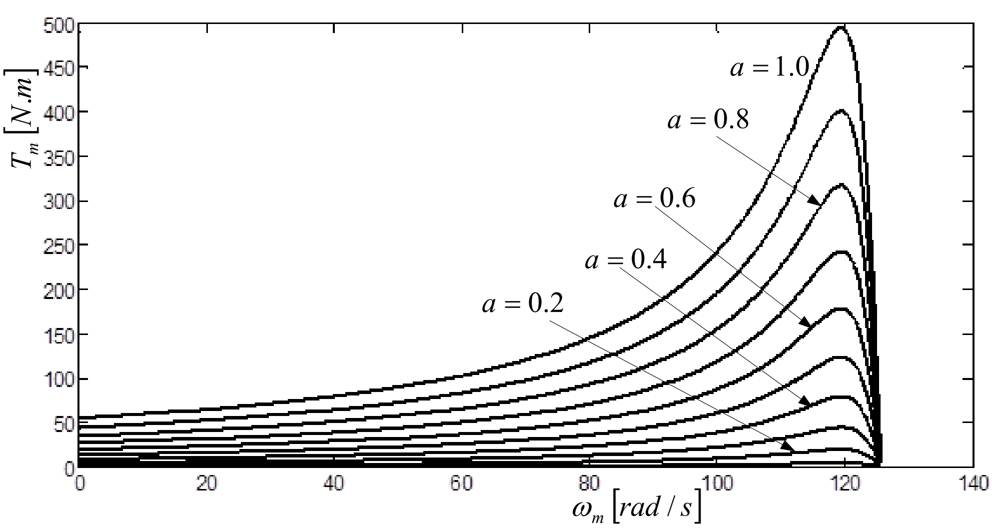

Figure 6: Torque - Speed characteristics for varying V_s

Figure 6 shows that speed and torque decrease with decrease in V_s. At starting, $\omega_m = 0$, $s = 1$. For all the various values of a, maximum torques occur at the same motor speed of 119.5 rad/s and maximum slip of 0.0498.

3.2 Frequency Control.

Synchronous speed is directly proportional to the supply frequency. If rated supply frequency is f_r then, $\omega_s = \dfrac{4\pi f_r}{p}$. Therefore, the synchronous speed and the motor speed can be controlled below and above the normal full-load speed by changing the supply frequency, while keeping the supply voltage V_s, constant at rated value. The equivalent circuit applied is shown in Figure 7.

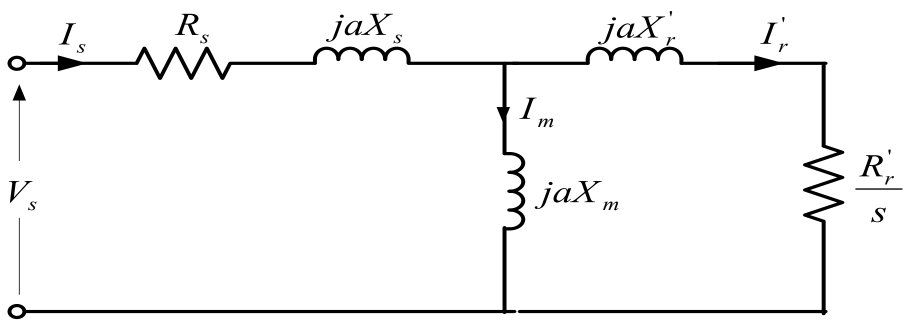

Figure: 7 Per phase equivalent circuit referred to the stator.

At another frequency, $f = a\,f_r$ (can be less or greater than 1)

$$Z_{in} = R_s + jaX_s + \frac{jaX_m\left(\frac{R_r^{'}}{s} + jaX_r^{'}\right)}{\frac{R_r^{'}}{s} + ja\left(X_m + X_r^{'}\right)} \tag{18}$$

$$a\omega_s = \frac{4\pi\, a\, f_r}{p} = \frac{2}{p} a\omega \tag{19}$$

$$s = \frac{a\omega_s - \omega_m}{a\omega_s} \tag{20}$$

$$\omega_m = a\omega_s\left(1 - s\right) = \frac{2}{p} a\omega(1 - s) \tag{21}$$

$$T_m = \frac{3p}{2\omega}\frac{R_s}{as} I_r^{'2} \tag{22}$$

Figure 8 and Figure 9 are the torque - speed characteristics for varying supply frequency (f_s).

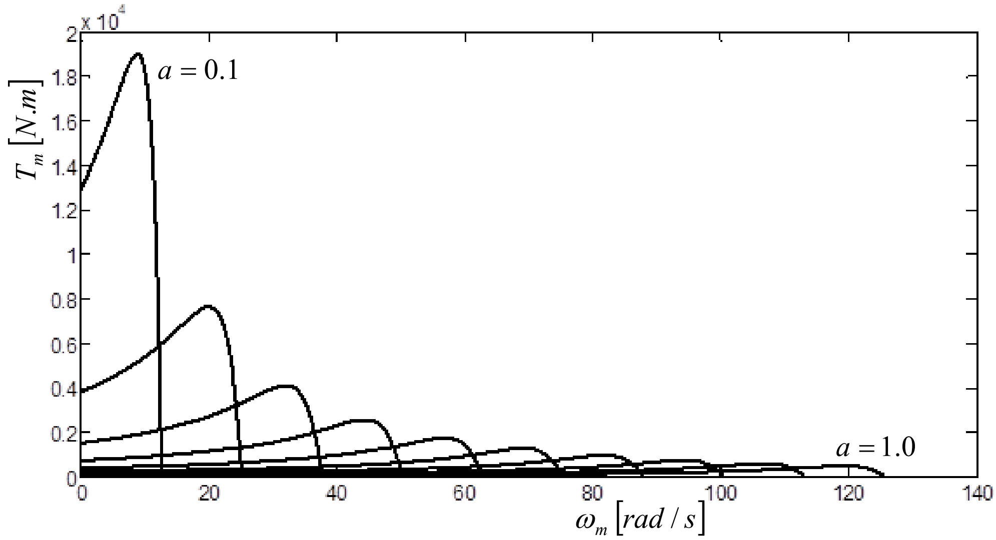

Figure 8: Torque - Speed characteristics for varying supply frequency (f_s) when $0 < a \leq 1$

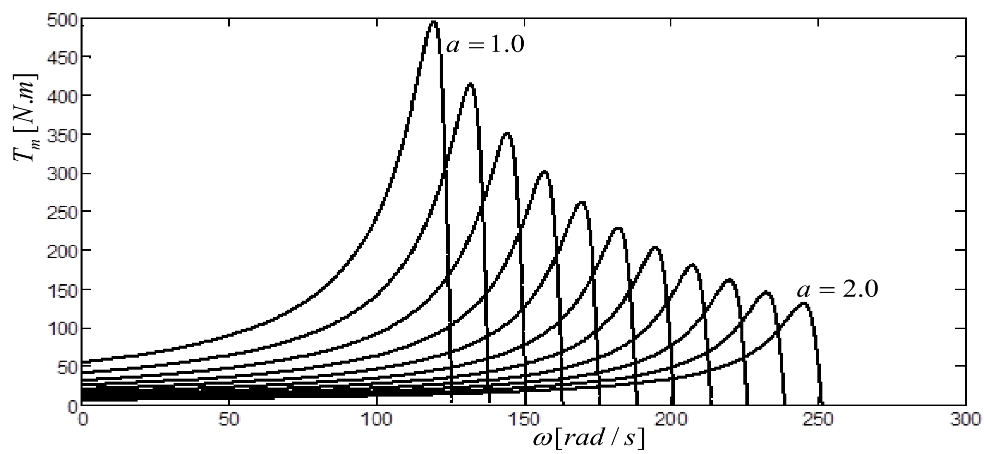

Figure 9: Torque - Speed characteristics for varying supply frequency (f_s) when $1.0 < a \leq 2.0$

Figure 8 and Figure 9 show that the torque tends to zero as a increases. For a given torque demand, the speed is controlled by changing the frequency. f_s is varied by adjusting the inverter switching frequency.

3.3 Voltage and frequency Control (constant flux control).

If the stator voltage drop is neglected, the voltage induced in the stator is equal to the supply voltage V_s [6]. Thus:

$$V_s = k\, f_s\, \phi \tag{23}$$

k = constant, ϕ = air-gap flux

$$\phi = \frac{V_s}{k\, f_s} \tag{24}$$

For the induction motor to operate, a smooth rotating air-gap flux is required (Bojan et al, 2012). From equation (24), any reduction in f_s without a change in V_s causes an increase in ϕ which will saturate the motor, leading to increase in magnetizing current, distortion of line current and voltage, core loss, stator copper loss, and production of high-pitched noise. However, decrease of ϕ should be avoided in order to retain the torque capability of the motor. Therefore, the variable frequency control below the rated frequency is generally carried out by reducing the machine supply voltage along with the frequency in such a manner that the flux is maintained constant. That is, the ratio $\frac{V_s}{f_s}$ is maintained constant at rated value. This is constant flux control or $\frac{V_s}{f_s}$ drive. Figure 10 is used for this analysis.

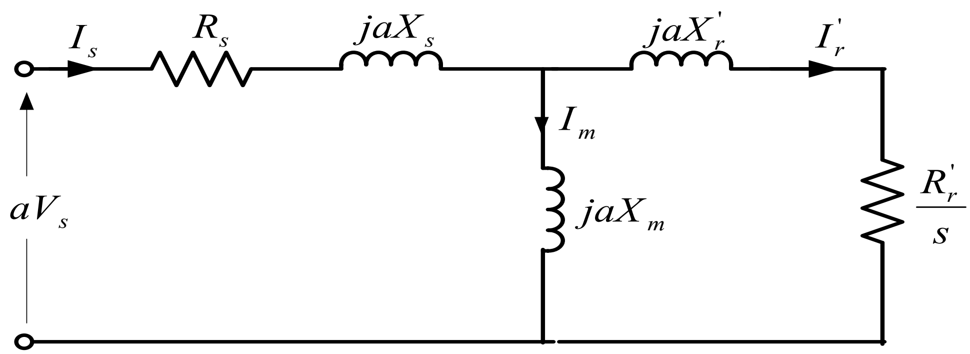

Figure 10: Per phase approximate equivalent circuit referred to the stator

$V = aV_s$ is applied to the stator at frequency $f = a\,f_r$, where $0 < a \le 1$

$$\omega_m = \frac{2}{p} a\omega(1-s) \tag{25}$$

$$T_m = \frac{3p}{2\omega}\frac{R_s}{as} I_r'^2 \tag{26}$$

The typical torque-speed characteristics are shown in Figure 11.

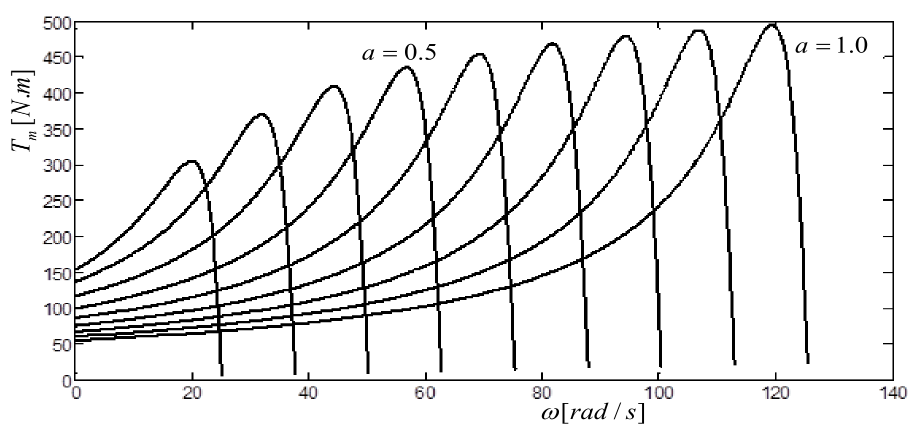

Figure 11 Torque - Speed characteristics for constant control

As a is increased, maximum torque tends to be constant. Conversely, maximum torque (Tmax) decreases as a or ωm decreases. By varying both the voltage and frequency, the torque and speed are controlled.

IV. CONCLUSION

In this paper, control of the speed and torque of squirrel-cage induction motor has been investigated. The control was implemented by three-phase fully-controlled rectifier and voltage source inverter. This is an ac-to-ac converter with a dc link. Three types of control were examined. However, the most efficient method is the voltage to frequency ratio control. This ratio is kept constant at its rated value. The flux is maintained constant, and the maximum torque, which is independent of frequency, can be maintained approximately constant. However at low frequencies, the air-gap flux is reduced due to the drop in the stator impedance and the ratio has to be increased to maintain the torque level.

REFERENCES

[1] Arbi G.S., Chetan G., Mohamed A.K., Barendse P. and Pragasen P. (2012). An Algorithm for Nonintrusive In Situ Efficiency Estimation of Induction Machines Operating With Unbalanced Supply Conditions. IEEE Transactions on Industry Applications, Vol. 48, No. 6: 2123-2130.

[2] Bojan S., Tine M. and Miralem H. (2012). Direct Comparison of Induction Motor and Line-Start IPM Synchronous Motor Characteristics for Semi-Hermetic Compressor Drives. IEEE Transactions on Industry Applications, Vol. 48, No. 6: 2310-2321.

[3] Daniel W.H. (1997). Introduction to Power Electronics. Prentice Hall, New Jersey: 291-328.

[4] Domentico C., Giovanni S., Angelo T., Luca Z. and Francesco P. (2003). Performance Analysis of a speed sensorless Induction Motor Drive Based on a constant-Switching frequency DTC Scheme. IEEE Transactions on Industry Applications, Vol. 39, No.2: 476-484.

[5] Dubey G.K. (1989). Power Semi-conductor Controlled Drives, Prentice Hall, N.J.: 203-300.

[6] Federico C., Fabio C. and Honorato H. (1998). Low-cost Compact Permanent Magnet Machine for Adjustable-Speed Pump Application. IEEE Transactions on Industry Applications, Vol. 34, No. 1: 109-116.

[7] Hubert H., Claudia M. and Gerard-Andre C. (2004). An Equivalent Internal Circuit of the Induction Machine for Advanced Spectral Analysis. IEEE Transactions on Industry Applications, Vol. 40, No.2: 726-734.

[8] John S. H., Kueck J.D., Mitchell O., Don A. C., Pedro J. O. and Leon M. T. (1998). Comparison of Induction Motor Field Efficiency Evaluation Methods. IEEE Transactions on Industry Applications, Vol. 34, No. 1: 117-125.

[9] Katsumi Y. and Yoshihisa H. (2004). Stray-load loss Analysis of Induction Motor-Comparison of Measurement due to IEEE standard 112 and Direct calculation by Finite-element method. IEEE Transaction on Industry Applications, Vol.40, No.2: 543-549.

[10] Miller T.J.E., Mirca P., Calnum C., Malcom M., Giovanni S., Nicola T. and Roberto S. (2004). Line-start Permanent-magnet Motor Single-phase Steady State Performance analysis. IEEE Transactions on Industry Applications, Vol. 40, No.2: 516-524.

[11] Muhammad H. R (1993). Power Electronics – Circuits, Devices and Applications. Prentice Hall, New Jersey: 542-567.

[12] Nkosinathi G. and Maarten J.K. (2012). Multiphase Cage-Rotor Induction-Machine Drive with Direct Implementation of Brush DC Operation. IEEE Transactions on Industry Applications, Vol. 48, No. 6: 2014-2021.

[13] Roozbeh N., Arash K.S. and Keyue M.S. (2016). Dual Flying Capacitor Active-Neutral-Point-Clamped Multilevel Converter. IEEE Transactions on Power Electronics, Vol. 31, No. 9: 6476-6484.

[14] Subhasis N., Shehab A., Hamid A. T. and Mohan R.B. (2003). Selection Criteria of Induction Machines for Speed Sensor less Drive Applications. IEEE Transactions on Industry Applications, Vol. 39, No.3: 704-712.

[15] Tsai-Fu. Wu (2016). Decoding and Synthesizing Transformerless PWM Conerters. IEEE Transactions on Power Electronics, Vol. 31, No. 9: 6293-6304.